

# ARRAY ELEMENT LOCALISATION OF RAPIDLY DEPLOYED SYSTEMS

Michael V. Greening

Defence Science and Technology Organisation,  
Salisbury Site, MOD Building 79, P.O. Box 1500,  
Salisbury, S.A., 5108, Australia,  
Email: mike.greening@dsto.defence.gov.au

## ABSTRACT

Array processing techniques such as beamforming or matched field processing require accurate knowledge of the location of individual elements in the array. For horizontal arrays laid on the ocean floor, relative arrival times measured across the array from nearby implosive sources are often used to aid in estimating the sensor positions. However, the inverse problem of determining the sensor positions from the relative arrival times is both nonunique and ill-conditioned. Standard grid search techniques rely on very accurate measurements of the source locations and some knowledge of the array. This paper shows how simulated annealing can be used to solve the inverse problem with limited knowledge of the array or source locations. Synthetic studies show that relative sensor locations can be exactly found while tests with real data show an improvement in array gain comparable to the theoretical limit obtained from a perfectly known array.

## RÉSUMÉ

Les techniques de traitement de signal de réseau, tel la conformation du faisceau et le traitement de champs appariés nécessitent une connaissance précise de la location des éléments individuels du réseau. Pour des réseaux horizontaux déployés sur le fond marin, les temps d'arrivée relatifs des signaux provenant de sources implosives proches, mesurés le long du réseau, sont souvent utilisés pour aider à l'estimation de la position des capteurs. Par contre, le problème inverse de la détermination de la position des capteurs à partir des temps d'arrivée relatifs est non-unique et mal défini. Les techniques de recherche sur une grille standard dépendent de la mesure très précise des positions de la source, et d'une première approximation de la position du réseau. Cet article démontre comment le traitement thermique simulé peut être utilisé pour résoudre le problème inverse avec une connaissance limitée de la position du réseau et de la source. Des études avec des données synthétiques démontrent que la position relative des capteurs peut être établie avec précision, et des essais avec des données réelles produisent une amélioration du gain de réseau comparable à la limite théorique pour un emplacement de réseau parfaitement connu.

## 1. INTRODUCTION

Remotely deployed systems often contain horizontal or vertical arrays mounted on the ocean floor and are used to acoustically monitor areas of the ocean. One problem with remotely deployed systems is accurately determining the sensor positions in the array. Conventional beamforming is often considered to require sensor position estimates accurate to within  $\lambda/10$  where  $\lambda$  is the wavelength of the signal measured.<sup>1</sup> More advanced array processing techniques such as adaptive beamforming or matched field processing require even more accurate estimates of the sensor positions.<sup>2,3</sup>

Sensor positions in remote systems are often estimated by measuring correlations from nearby continuous sources,<sup>4,5</sup>

or by measuring arrival times from nearby transient sources.<sup>6-9</sup> For transient sources, if the location of the sources and the travel times to the sensors are known, then the location of all the sensors in the array can be unambiguously determined using triangulation from three sources. However, the source locations are often only known approximately and the travel times from source to sensor are often unknown with the arrival times at any sensor only known relative to the arrival times at other sensors. The inverse problem of estimating the sensor positions from relative arrival times with unknown source locations is nonlinear (the radial distance between a source and sensor depends linearly on the arrival time but the sensor position also depends on the bearing to the source), nonunique (unknown source positions can allow for a rotation or translation of the combined system of sources and sensors without a change in the arrival times), and may be ill-conditioned depending on the

source and sensor geometry<sup>10</sup> (a small error in a source position can lead to a large error in a sensor position).

One method of solving the nonlinear inverse problem is to transform it into a linearised problem and iterate towards a solution based on an initial starting model.<sup>6,8,9</sup> However, this is often found to be highly dependent on the initial estimate of the source locations. Another way to find the sensor positions from unknown source positions is simply to search a multidimensional space of estimated sensor and source positions and minimize the error between the measured and predicted relative arrival times. One technique designed specifically to search ill-conditioned, multidimensional spaces is called simulated annealing.<sup>11</sup> Although simulated annealing is also an iterative technique, it is not highly dependent on the initial estimate of the unknown parameters. This is important if source positions cannot be measured accurately, such as for sources at depth or if GPS is not available. Other authors have already used simulated annealing to localize a small vertical array with few sensors.<sup>6</sup> This paper will show that simulated annealing can be applied to the problem of locating a large horizontal array with many sensors and only a limited knowledge of the source locations.

## 2. EXPERIMENT

The data analyzed in this paper were collected during the RDS-2 trial in November 1998 in 107 m water in the Timor Sea off the northern coast of Australia at 12° 20' S, 128° 20' E. Bathymetric surveys show the area to be very flat with changes of depth of only several meters over several kilometers. A sound speed profile obtained using an XBT indicated a piecewise linear profile with a sound speed at the surface of 1549 m/sec, decreasing to 1544.5 m/sec at 75 m depth, and then increasing to 1545.5 m/sec at 107 m depth. The measured sound speed profile was used in estimating sensor positions for the real data.

The data examined were collected on the ULITE array deployed by the Space and Naval Warfare Systems Center (SPAWAR), San Diego, CA., USA. The planned deployment of the ULITE array and light bulb sources<sup>12</sup> is shown in Fig. 1. The array is a horizontal array which lies on the ocean floor and consists of three arms of 32 sensors each, tied in the center, with each arm containing a slight curvature to break the left/right symmetry from the arm. The sensors in each arm of the array are asymmetrically nested for three different design frequencies of 24, 48 and 96 Hz., resulting in sensor separations of 8, 16 and 32 m for sensors 1-17, 17-25 and 25-32 respectively. All light bulbs were imploded at 55 m depth with the planned locations to include three light bulbs on each side of each arm, approximately 100 m distance from the arm.

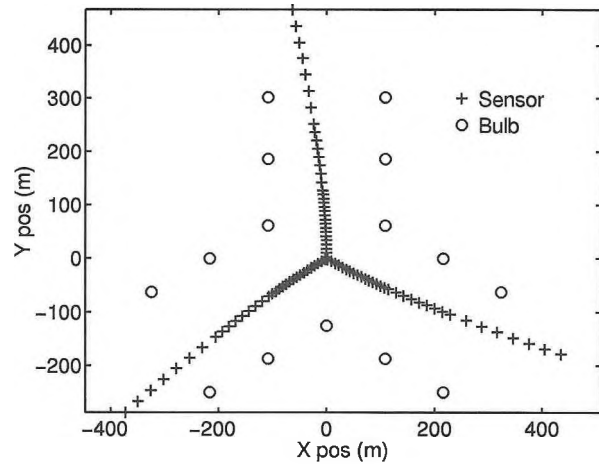


Figure 1: Trial layout plan.

The array was deployed using three boats which met at the center location for the array, then moved apart, each boat deploying one arm of the array. To keep the array from breaking, slow boat speeds were required to ensure low tension on the cables. The slow boat speeds, low cable tension, and high currents of two knots resulted in the deployment pattern of the array differing significantly from the planned deployment. The estimated array shape of the actual deployment is given in Sec. 4.

## 3. METHODOLOGY

This section shows how to apply simulated annealing to the problem of locating a horizontal array mounted on the ocean floor. A set of transient sources are used near mid-depth and the relative arrival times of the direct arrival and surface reflection are measured across the array. The problem then is to use simulated annealing to find a set of source and sensor locations which will reproduce the relative arrival times.

Simulated annealing involves a series of iterations in which the unknown parameters (ie. source and sensor locations) are perturbed. For each iteration, the relative arrival times of the direct arrival and surface reflection are calculated for the modelled parameters. The modelled arrival times are then compared with the measured arrival times and the total time error  $E$  is given as an estimate of the goodness of fit of the modelled source and sensor positions to their true values. For successive iterations, the change in error  $\Delta E$  is calculated. If the error has decreased ( $\Delta E < 0$ ), the new parameter configuration is accepted. If the error has increased ( $\Delta E > 0$ ), the new configuration has a probability  $P$  of being accepted with the probability being drawn from the Boltzmann distribution:

$$P(\Delta E) = \exp(-\Delta E/T), \quad (1)$$

where  $T$  is a controlling parameter analogous to temperature in the physical process of annealing. Accepting some

perturbations which increase  $E$  allows the algorithm to escape from local suboptimal minima in the search space. Decreasing  $T$  with successive iterations decreases the probability of accepting an increase in error, and the algorithm eventually converges to a solution which should approximate the global minimum.

Two factors involved in developing an efficient and effective simulated annealing algorithm are the method of decreasing the temperature  $T$ , and the method of perturbing the unknown parameters. A starting temperature  $T_0$  was chosen which allows at least 90% of all perturbations to be accepted. This ensures that the final result does not depend on the starting estimate of the unknown parameters. A number of perturbations  $h$  are then performed before decreasing the temperature according to  $T_{j+1} = \alpha T_j$ , where  $\alpha < 1$ . The process is terminated when further temperature steps do not result in a lower error or when the error is within an acceptable margin. The values of  $\eta$  and  $\alpha$  to use depend on the difficulty of the inversion. Increasing both  $\eta$  and  $\alpha$  should decrease the final error but also increases the number of iterations and time required. An estimate of  $\eta$  and  $\alpha$  can be obtained by using synthetic data and choosing  $\eta$  and  $\alpha$  large enough that the final error is zero or the resulting sensor locations are accurate to within an acceptable tolerance. With real data,  $\eta$  and  $\alpha$  can be initialized to the values obtained from the synthetic study and then allowed to increase until there is no further decrease in the final error.

The method of perturbing the parameters can have a major effect on the efficiency of simulated annealing. Changing only one parameter at a time allows the algorithm to converge for a sensitive parameter while continuing to search for less sensitive parameters. Changing multiple parameters in one perturbation allows for quicker convergence when coupled parameters are involved and also allows for easier jumping between local minima. Also, a parameter may be changed in different ways. In the algorithm used, when changing a parameter, either a new value is picked within a Gaussian distribution centered on the current value (allowing convergence towards a solution) or a new random value is chosen from the entire allowable range for that parameter (allowing escape from local minima).

After the simulated annealing algorithm stops, a gradient descent algorithm was applied using the result of the simulated annealing as the initial estimate. This is used to ensure that the absolute minimum of the current trough is found.

#### 4. RESULTS

For our problem, the unknown parameters used are the source and sensor locations along with the bottom depth. For every perturbation a source, sensor or bottom depth is ran-

domly chosen to be changed. If a source is picked, the position (in  $x, y$  and  $z$ ) of only a single source is changed for a given perturbation. If a sensor is picked, either a single sensor, multiple sensors or the entire array can be changed in the following manner. The entire array can be changed by shifting it horizontally or by rotating it about some angle. A single sensor can be changed by changing its distance or bearing from the previous sensor without moving other sensors, providing that the separation between pairs of sensors does not exceed the length of cable joining them. Multiple sensors can also be changed by moving all sensors before or after a given sensor by the same change given to that sensor. For both the synthetic and real data studies, a flat bottom is assumed with all sensors considered to be at the bottom depth.

Using Fig. 1 to generate synthetic data, the simulated annealing algorithm was tested with the following uncertainties: the center of the array was assumed to be known to within 100 m; the bearing or range from one sensor to the next was unrestricted except that the range between a pair of sensors could not be greater than the length of cable separating them; the horizontal position of a source was assumed to be known within 100 m; the depth of a source was assumed to be known within 20 m; the water depth was assumed to be known within 20 m. Although the uncertainties are larger than the true uncertainties in the real data, using large uncertainties helps demonstrate the robustness of the technique. With the above uncertainties, if the relative arrival times were known exactly (ie. not digitised), then the relative array shape and light bulb positions were found within  $10^{-2}$  m. If the relative times were only known within a digitisation sample, then the relative position of any sensor could shift from its true relative position by as much as the distance travelled by sound within the time of the digitisation sample. Increasing the number of light bulbs decreases the positional shift introduced by the digitisation.

The relative arrival times of the direct arrival and surface

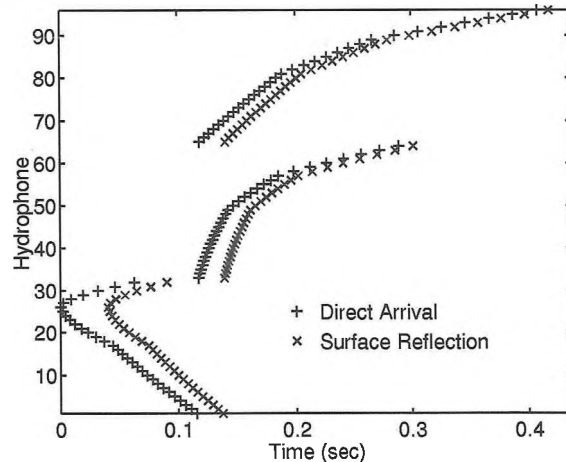


Figure 2: Relative arrival times.

reflection for synthetic data using the light bulb at (100 m, 300 m) are shown in Fig. 2. In this figure, hydrophone numbers 1-32 represent the north arm, numbers 33-64 represent the south-east arm, and 65-96 represent the south-west arm.

For the real data, The estimated source positions and array shape of the ULITE array as determined by both DSTO and SPAWAR are shown in Fig. 3. Although the shape differs significantly from the planned deployment, this is believed to be due to the high currents and the requirement to deploy the array at low speed without cable tension. The reason for the change in light bulb positions from the trial plan is simply because the array was known to have deviated from the trial plan but could not be accurately estimated on site. Thus, an estimate of where to deploy the light bulbs had to be made without accurate knowledge of the array position. The similarity of array shape estimated by DSTO and SPAWAR provides some confidence that the correct shape was obtained. The SPAWAR estimate used a grid search technique to find the hydrophone locations assuming a fixed bottom depth of 107 m and fixed light bulb locations at 55 m depth and at the recorded GPS positions. The simulated annealing technique used at DSTO allowed uncertainties of 20 m in the bottom depth, along with uncertainties of 100 m in the horizontal location and 20 m in the depth of a light bulb. The simulated annealing algorithm returned a bottom depth of 107.2 m and depths of 48-55 m for all light bulbs.

For individual arms of the array, the relative shapes estimated by DSTO and SPAWAR are very similar as shown in Fig. 4. The main difference in the estimates of the individual arms is that the SPAWAR estimates show smoother array arm shapes than the DSTO estimates. This is largely because the SPAWAR estimate only included the 16 sensors in each arm spaced by 32 m while the DSTO estimate included every sensor in all arms of the array. The roughness in array arm shapes shown by the DSTO estimate is believed to exist in the real array. If the array arms were deployed under tension, then this roughness would not be expected and an

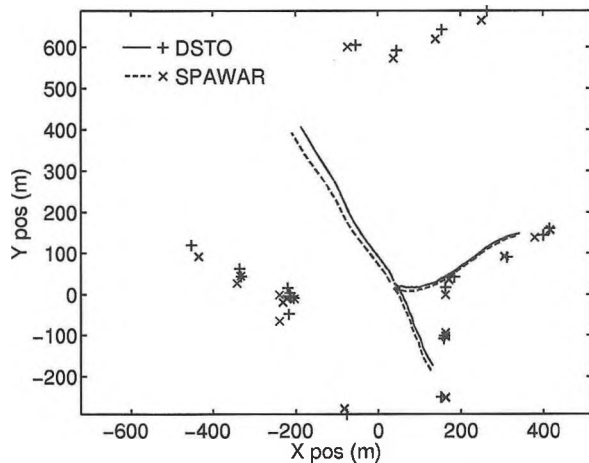


Figure 3: Estimated trial layout.

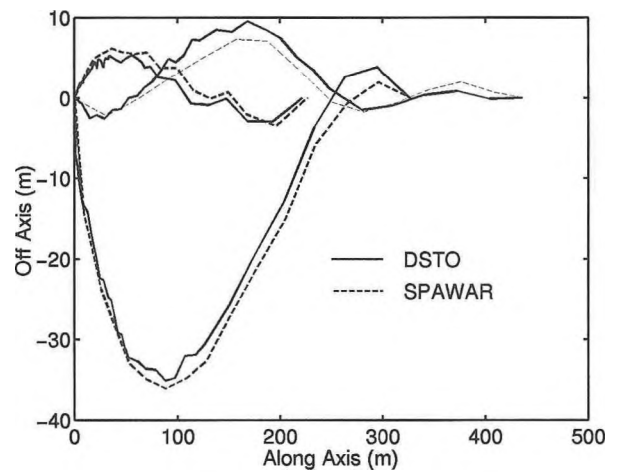


Figure 4: Estimated shapes of array arms.

inversion technique which would minimize the array curvature should be used.<sup>8</sup>

Although the relative shapes of individual arms are very similar, the relative shapes of the entire array show a difference of a 2° rotation in the direction of the northward pointing arm relative to the other two arms. The reason for the difference between the two estimated shapes is believed to be caused by the location of the light bulbs, which were not as tightly concentrated along the arms of the array as in the trial plan. Consider a light bulb which is near endfire to one arm and near broadside to another. A shift in the light bulb position can cause a large change in the relative arrival times across the broadside array but very little change across the endfire array. Thus, having many light bulbs near endfire of one arm can cause a relative shift in the heading between two arms of the array with little difference in the relative arrival times. This is the case for the ULITE deployment which has a large number of sources, the light bulbs west of the array, that are near endfire to the east arm of the array and near broadside to the north arm of the array.

When the uncertainty in the horizontal positions of the light bulb sources was reduced from 100 m to 10 m, the shape of the individual arms remained nearly identical and the rotation difference in the north arm of the array as estimated by DSTO and SPAWAR disappeared. This gives good confidence in the shape of individual arms of the array, but does not necessarily indicate which of the headings for the north arm of the array is correct. To determine this, the errors between the measured and modelled arrival times for the estimated source and sensor positions must be examined.

The errors between the measured and modelled arrival times are shown in Fig. 5 for the case when source positions are only known within 100 m. Each horizontal line shows the error in arrival times for both the direct arrival and surface reflection from all light bulbs. Nearly all errors fall within

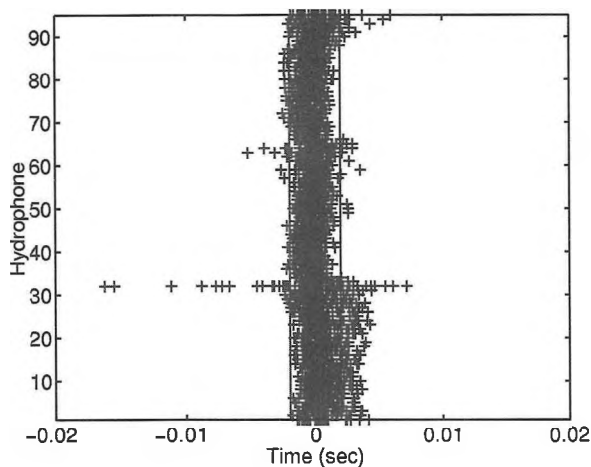


Figure 5: Arrival time errors.

the digitisation sample size of 0.002 sec, with the average error being 0.0009 sec per arrival (0.45 digitisation samples). This provides further confidence that the true array shape is well approximated. Sensor 32 is the outermost sensor on the northward pointing arm of the array and was connected to a surface buoy. It is believed that the buoy was causing this sensor to move and thus, an accurate estimate of its position could not be found, and it contains large errors in the arrival time estimates. This was also found by SPAWAR. This sensor is not plotted in Figs. 3 or 4.

When the uncertainty in the source locations was decreased to 10 m, the average error fell to 0.0007 sec per arrival (0.34 digitisation samples), and nearly all errors larger than the digitisation sample size occurred either for the first three light bulb sources measured on the north arm of the array, or for sensor number 32. The smaller error obtained using the tighter bounds on the light bulb positions indicates that this is likely a better estimate of the heading of the north arm of the array than that determined from the loose bounds on the light bulb positions. However, the larger errors obtained for the north arm of the array than for the east or south arms indicate that the north arm of the array may not be estimated as well as the other two arms. This was consistent using tight or loose bounds on the light bulb positions. The larger error in the shape of the north arm is believed to be caused both by the buoy which may be dragging that arm of the array in the high currents, and by the lack of nearby light bulb sources along the length of this arm of the array. Both the east and south arms have multiple light bulbs within 50 m of the hydrophones while the closest light bulb to the north arm is over 200 m away.

Determining the number and location of light bulbs required to accurately estimate an array shape is array dependent. A study of a single, nearly linear array of 200 m length showed that four light bulbs with two along one side, one along the other side and one near endfire always provided solutions

accurate to within the distance travelled by sound within the time of the digitisation sample, provided that the light bulbs were within 200 m of the array. A more complete analysis of optimal source locations is available in Dosso and Sotirin.<sup>10</sup>

A final indication of the accuracy of the estimated array shape can be obtained by beamforming on real data that contains only a single target with a large snr. Under this condition, the total energy measured across the array (or averaged into a covariance matrix) should be reproduced when beamforming at the target location. During the trial, an 80 Hz tonal target was deployed at 100° relative to North and 3200 m from the center of the array. The conventional beamformer reproduced 80%, 97%, 97% and 75% of the total power measured across the north arm, east arm, south arm and full array respectively when steered at this target. This represents a loss of only 1.0 dB, 0.1 dB, 0.1 dB and 1.2 dB respectively. Thus, the shapes of the east and south arms are assumed to be very accurately estimated while the north arm still contains some error. This was also indicated in Fig. 5 which showed that the largest arrival time errors were from the north arm.

The beamformed output of each individual arm of the array and of the full array is shown in Fig. 6. This figure shows the results of conventional focussed beamforming on the real data (solid line), conventional focussed beamforming on synthetic data for a source at the known target location and in infinitely deep water (dashed line), and adaptive focussed beamforming on the real data (dotted line). The minimum variance distortionless response (mvdr) beamformer was used as the adaptive beamformer. The close agreement between the real and synthetic data for the east and south arms again shows that the shapes of these arms are well estimated. The close agreement also indicates that very little signal loss occurs due to the multipath effects of the shallow water environment for this frequency and range. Finally, the shapes of the east and south arms are estimated accurately enough to give good performance for the adaptive beamformer, which is known to be highly sensitive to errors in the array shape.<sup>2</sup> Note that the adaptive beamformer nearly eliminates the large sidelobes of the conventional beamformer. Although the adaptive beamformer still returns the correct signal directions for the north arm and the full array, the array gain is poor.

## 5. SUMMARY

This paper has shown how simulated annealing can be used to accurately perform array element localisation on remotely deployed systems. Synthetic studies have shown that the relative sensor positions can be determined within the distance travelled by sound during the time of the digitisation sample size if sufficient light bulbs are employed nearby along the

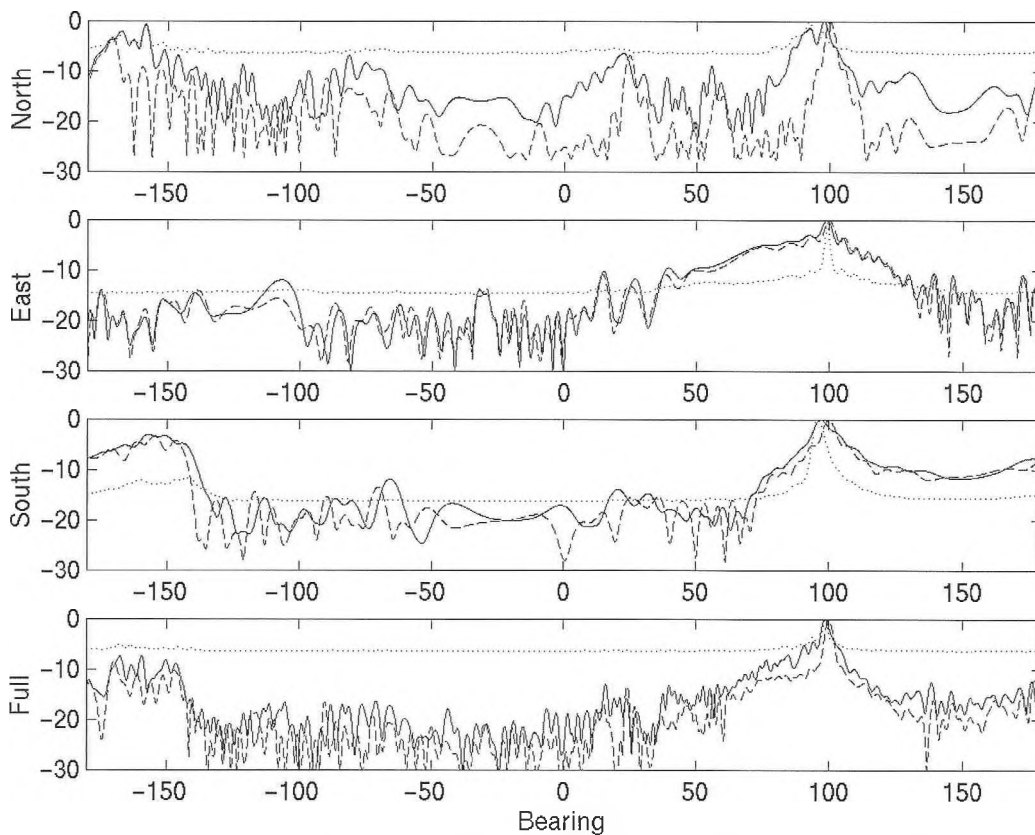


Figure 6: Beamformed output (in dB) of the north arm, east arm, south arm and full array. Results show the conventional beamformer on real data (solid line), the conventional beamformer on synthetic data with a target at the known true target location (dashed line), and the mvdr adaptive beamformer on real data (dotted line). The true target is at  $100^\circ$ , 3200 m.

array and at endfire to the array. Although ground truth was not available on the real data trial, there are four indications that the array shape is well estimated. These are: agreement with an independently performed localisation estimate; reproduction of up to 97% of the total energy measured across an individual arm of the array when beamformed at a dominant source; close agreement between the beamformed results for real data and for synthetic data using a single target at the known source location; and finally, good beamforming performance using the adaptive beamformer which is known to be sensitive to errors in array shape.

## 6. ACKNOWLEDGEMENTS

The author would like to gratefully acknowledge the Space and Naval Warfare Systems Center in San Diego, CA, USA for the use of the ULITE data and for the collaboration in comparing array element localisation results.

## 7. REFERENCES

1. B.D.Steinberg, *Principles of Aperture and Array System Design*, Wiley, New York, 1976.
2. S.D.Hayward, "Effects of motion on adaptive arrays," *IEE Proc.: Radar, Sonar and Navigation*, **144**, (1), 15-20, (1997).
3. H.Schmidt, A.B.Baggeroer, W.A.Kuperman, and E.K.Scheer, "Environmentally tolerant beamforming for high-resolution matched field processing: Deterministic mismatch," *J.Acoust.Soc.Am.*, **88**, 1851-1862, (1990).
4. K.C.Creager and L.M.Dorman, "Location of Instruments on the Seafloor by Joint Adjustment of Instrument and Ship Positions," *J.Geophys.Res.*, **87**, (B10), 8379-8388, (1982).
5. C.H.Knapp and G.C.Carter, "The Generalized Correlation Method for Estimation of Time Delay," *IEEE Trans.Acoustics, Speech and Signal Proc.*, **24**, (4), 320-327, (1976).
6. G.H.Brooke, S.J.Kilistoff, and B.J.Sotirin, "Array Element Localization Algorithms for Vertical Line Arrays," *Proceedings of the 3<sup>rd</sup> European Conference on Underwater Acoustics*, edited by J.S.Papadakis, Crete U.P., Heraklion, 537-542 (1996).

7. W.S.Hodgkiss, D.E.Ensberg, J.J.Murray, G.L.D'Spain, N.O.Booth and P.W.Schey, "Direct Measurement and Matched-Field Inversion Approaches to Array Shape Estimation," IEEE J.Ocean Eng., **21** (4), 393-401, (1996).
8. S.E.Dosso, M.R.Fallat, B.J.Sotirin and J.L.Newton, "Array element localization for horizontal arrays via Occam's inversion," J.Acoust.Soc.Am., **104**, (2), 846-859, (1998).
9. S.E.Dosso, G.H.Brooke, S.J.Kilistoff, B.J.Sotirin, V.K.McDonald, M.R.Fallat and N.E.Collison, "High-Precision Array Element Localization for Vertical Line Arrays in the Arctic Ocean," IEEE J.Ocean Eng., **23** (4), 365-378, (1998).
10. S.E.Dosso and B.J.Sotirin, "Optimal array element localization," J.Acoust.Soc.Am., **106**, (6), 3445-3459, (1999).
11. S.Kirkpatrick, C.D.Gelatt, and M.Vecchi, "Optimization by Simulated Annealing," Science **220**, 671-680, (1983).
12. G.J.Heard, M.McDonald, N.R.Chapman, and L.Jaschke, "Underwater light bulb implosions: a useful acoustic source," Oceans 97. MTS/IEEE. Conference Proceedings. IEEE Part 2, vol 2, 755-762, (1997).

### ANNOUNCEMENT

To all my colleagues:

Many of us perform both acoustic and vibration work. Obviously, those of us in the acoustic side are members of the CAA. We interact with our peers by reading the journal and attending the annual meeting. For the vibration side, I would like to suggest participation in the Canadian Machinery Vibration Association, **CMVA**. There are regular Chapter meetings across Canada, with two chapters here in Ontario (Central and Eastern). For further information see the website [www.cmva.com](http://www.cmva.com), or call me directly.

Chris Hugh  
 Chair - Central Ontario Chapter  
 CMVA Central Ontario Chapter  
 Acoustics & Vibration  
 Tel: (905) 403-3908  
 email: [chugh@hatch.ca](mailto:chugh@hatch.ca)

# J.P. ENVIRONMENTAL

## NOISE AND VIBRATION CONTROL PRODUCTS

At J.P. Environmental we pride ourselves on analyzing your noise and vibration control problem, and recommending the solution that best suits your needs. In our plant, we manufacture your equipment to your specifications, while always maintaining high quality and prompt service – *BEFORE, DURING* and *AFTER* delivery.

### PRODUCTS WITH A PROVEN TRACK RECORD

*HEAVY DUTY INTAKE AND DISCHARGE SILENCERS...*for power generation, industrial and ventilation fans, and other equipment up to 1,000,000 cfm and 1000°F.

*EXHAUST STACK SILENCERS...*for high velocity and high temperature applications - carbon steel, stainless steel, Hastaloy and FRP construction.

*VENT AND BLOWDOWN SILENCERS...*to control high pressure jet noise from steam, natural gas and air, in-process, safety and dumping valves.

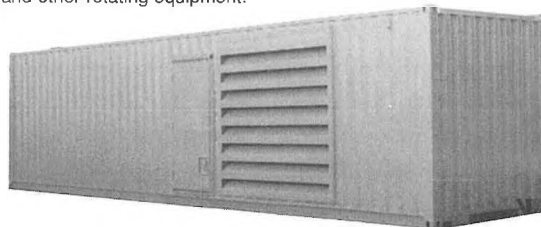
*HEAVY DUTY REACTIVE AND ABSORPTIVE MUFFLERS...*for any size diesel engine compressor, vacuum pump or positive displacement blower.

*COMPLETE ACOUSTICAL AND THERMAL ENCLOSURES...*ISO container, mobile, walk-in, drop-over and knockdown designs. Engineered, proven and hassle-free.

*FLEXIBLE CONNECTIONS AND EXPANSION JOINTS...*to eliminate duct vibration on equipment intakes and outlets. Acoustic designs are also available.

*FILTER UNITS AND INLET FILTER BOXES...*for building ventilation and fan intake systems. All engineered and built to meet the specific needs of the application.

*ISOLATORS AND ISOLATION/INERTIA BASES...*designed to reduce vibration from fans, pumps, compressors and other rotating equipment.



**J.P. Environmental Products Inc.**

P. O. Box 816, Stn. "C", Kitchener, Ontario, Canada N2G 4C5  
Tel: (519) 821-1199 Fax: (519) 821-2745 Toll Free: 1-800-663-4874 (HUSH)  
E-mail: [general@jpenvironmental.com](mailto:general@jpenvironmental.com)